

# Environment-Driven Emergence of Higher-Order Collective Behavior

Felipe S. Abril-Bermúdez,<sup>1,\*</sup> David N. Fisher,<sup>2,†</sup> Jean-Baptiste Gramain,<sup>1,‡</sup> and Francisco J. Pérez-Reche<sup>1,§</sup>

<sup>1</sup>*School of Natural and Computing Sciences, University of Aberdeen, Aberdeen AB24 3UE, United Kingdom.*

<sup>2</sup>*School of Biological Sciences, University of Aberdeen, Aberdeen, AB243FX, United Kingdom*

(Dated: February 18, 2026)

Collective behavior is commonly attributed to direct interactions among system components. Using a minimal stochastic model, we show that higher-order collective structure can instead emerge from shared stochastic environments, even in the absence of interactions. Quantified via the O-information, environmental fluctuations induce both redundant and synergistic dependencies, with the latter occupying larger regions of the correlation space. We establish a no-go theorem showing that time-independent coupling between the system variables and a shared stochastic environment rules out synergistic higher-order behavior. Crucially, this constraint can be overcome dynamically: transitions between redundancy and synergy arise from time-dependent environmental coupling or from the nontrivial interplay between shared environments and direct interactions. Together, these results identify environmental mediation as a distinct mechanism of higher-order collective organization beyond the conventional interaction-centric paradigm.

Keywords: Higher-order interactions, O-information, synergy, stochastic dynamics

Collective behavior in complex systems has often been described as emerging from simple local interactions at smaller characteristic scales [1, 2]. A defining hallmark of complexity, however, is that the behavior of the whole cannot be inferred from its parts, owing to collective dependencies that extend beyond pairwise correlations [3, 4]. Understanding how such higher-order structure emerges from microscopic interactions remains a central challenge across disciplines [5–9].

Early modeling efforts of complex systems focused on phenomena driven by pairwise interactions between elementary units [10, 11]. However, higher-order interactions, involving dependencies among three or more variables, are now recognized as fundamental to the structure and function of complex systems, from neural activity and biological phenomena to social and financial dynamics [5, 12–22].

Information-theoretic approaches provide a principled framework to connect the interaction mechanisms among elementary units with the collective behaviors that emerge at the system level by quantifying statistical dependencies that go beyond pairwise correlations. In particular, the O-information,  $\Omega$ , offers a compact measure of the balance between integration and segregation in a system [13]: positive values ( $\Omega > 0$ ) indicate redundancy-dominated regimes, where variables share overlapping information, whereas negative values ( $\Omega < 0$ ) signal synergy-dominated regimes, where collective effects convey information not present in any part alone—a quantitative expression of Anderson’s “more is different” principle [3].

The emergence of complex system behavior has typically been described in terms of deterministic interactions among elementary constituents. However, in both natural systems and artificial settings, these interacting units are rarely isolated: neurons, species, or agents often experience common environmental fluctuations that

modulate their dynamics and induce correlations or synchronization [23–26].

Here, we show that shared stochastic environments can themselves generate both synergistic and redundant higher-order behaviors, even in the absence of direct interaction between units. We further show that the combined effect of coupling to a shared environment and direct interactions leads to counterintuitive system behavior.

We study a minimal stochastic model describing the time evolution of three variables,  $\mathbf{z}(t) = \{z_1(t), z_2(t), z_3(t)\}$ , representative of a broad class of systems composed of interacting degrees of freedom subject to both idiosyncratic fluctuations and shared environmental forcing. Depending on the context, the variables  $\mathbf{z}$  may represent species abundances [24, 26], neural membrane potentials [27], or coarse-grained magnetization variables (soft spins) [28]. The model reveals a sharp geometric boundary in correlation space that separates redundant and synergistic regimes. This geometric perspective provides a direct link between stochastic dynamics [29], correlation structure, and emergent higher-order behavior.

We identify correlation-sign motifs sufficient for synergistic or redundant environment-driven collective behavior and show that synergy occupies larger regions of the correlation space. At the same time, we establish a no-go theorem demonstrating that synergistic higher-order organization cannot arise under static coupling to a shared environment.

Crucially, we observe transitions from redundancy to synergy when time-dependent environmental fluctuations are introduced or when the system variables are coupled via a tunable deterministic higher-order interaction. Taken together, these two mechanisms expand the traditional framework of complex systems, revealing a more nuanced landscape of collective organization.

*The model.*— The time evolution of the variables  $\mathbf{z}(t)$  is governed by deterministic interactions and stochastic environmental factors (see Fig. 1). More explicitly, we consider three Langevin degrees of freedom coupled to independent local baths and driven by a shared fluctuating field, governed by the following equations:

$$dz_1(t) = \mu_1 dt + \theta_1 dW_1(t) + f_1(t) dW(t) + m(\mathbf{z}) dt, \quad (1)$$

$$dz_2(t) = \mu_2 dt + \theta_2 dW_2(t) + f_2(t) dW(t), \quad (2)$$

$$dz_3(t) = \mu_3 dt + \theta_3 dW_3(t) + f_3(t) dW(t), \quad (3)$$

Here,  $W(t)$  represents the random effect of a shared global environment modeled by a Wiener process, and  $\{W_k(t)\}_{k=1}^3$  denote independent local noise sources acting on each variable. The functions  $\mathbf{f} = \{f_1(t), f_2(t), f_3(t)\}$  modulate the instantaneous coupling strength to the shared environment. The real-valued parameters  $\boldsymbol{\mu} = \{\mu_1, \mu_2, \mu_3\}$  correspond to the drift. The non-negative coefficients  $\boldsymbol{\theta} = \{\theta_1, \theta_2, \theta_3\}$  quantify the coupling to the local noise, which is assumed to be constant. The function  $m(\mathbf{z})$  encodes a deterministic interaction mechanism affecting  $z_1(t)$ , defined as follows:

$$m(\mathbf{z}) = m_1 e_1(\mathbf{z}) + m_2 e_2(\mathbf{z}) + m_3 e_3(\mathbf{z}). \quad (4)$$

Here,  $e_1(\mathbf{z}) = z_1 + z_2 + z_3$ ,  $e_2(\mathbf{z}) = z_1 z_2 + z_1 z_3 + z_2 z_3$ , and  $e_3(\mathbf{z}) = z_1 z_2 z_3$  are the elementary symmetric polynomials. The parameters  $m_1, m_2, m_3 \in \mathbb{R}$  decompose deterministic interactions into single (additive), pairwise, and genuine triplet interactions among the stochastic variables, respectively.

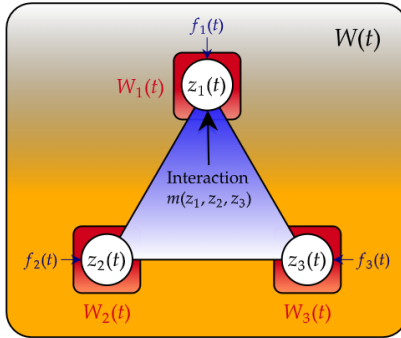


Figure 1. System composed of three elements with state variables  $z_1(t)$ ,  $z_2(t)$ , and  $z_3(t)$ . The evolution of all elements is affected by a shared global environment represented by a stochastic process  $W(t)$  and by local environment factors  $W_1(t)$ ,  $W_2(t)$ , and  $W_3(t)$ . The functions  $\{f_k(t)\}_{k=1}^3$  quantify the coupling strength between each element and the global environment. The dynamics of the first element include a deterministic interaction term  $m(\mathbf{z})$  capturing the interaction with itself and the other two elements.

The proposed model involves nonlinear couplings and multiplicative noise, precluding a closed-form analytical solution. We considered two complementary ap-

proaches. (i) Analytical results, based on the probability density function (PDF) of the joint stochastic process  $\mathbf{z}(t)$  (App. B in [30]). In this case, statistical observables such as the O-information are computed directly from the time-dependent PDF. (ii) Numerical simulations, which allow individual realizations of the stochastic dynamics to be examined. These are obtained by numerically integrating the stochastic system in Eqs. (1)–(3) using the Euler–Maruyama algorithm [31]. The O-information in the numerical simulations was estimated using the *HOI* Python toolbox [32].

*Effects of fluctuating environments in non-interacting systems.*— We first establish a fundamental constraint on purely stochastic collective organization. For non-interacting systems ( $m(\mathbf{z})=0$ ) with constant coupling to a shared environment, the emergence of synergy is forbidden, as formalized by Theorem C.1. in [30]. In this regime, one can show analytically that  $\mathbf{z} \sim \mathcal{N}(\mathbf{M}, \mathbf{C})$ , i.e.  $\mathbf{z}$  follows a multivariate Gaussian distribution (App. A in [30]), with mean vector  $\mathbf{M} = (\mu_1 t, \mu_2 t, \mu_3 t)^T$  and covariance matrix  $\mathbf{C}$  whose elements are given by (App. B in [30])

$$C_{kl}(t) = \delta_{kl} \theta_k \theta_l t + \int_0^t f_k(\tau) f_l(\tau) d\tau. \quad (5)$$

The O-information admits a closed-form expression (App. A in [30]):

$$\Omega(\mathbf{z}) = \frac{1}{2} \log_2 \left( \frac{1 + 2\rho_{12}\rho_{13}\rho_{23} - \rho_{12}^2 - \rho_{13}^2 - \rho_{23}^2}{(1 - \rho_{12}^2)(1 - \rho_{13}^2)(1 - \rho_{23}^2)} \right), \quad (6)$$

where  $\rho_{ij}(t) = C_{ij}/\sqrt{C_{ii}C_{jj}}$  are correlation coefficients.

The condition  $\Omega = 0$  induces a geometric partition of the correlation space  $[-1, 1]^3$  into regions of redundant ( $\Omega > 0$ ) and synergistic ( $\Omega < 0$ ) collective behavior. In practice, the zero-O-information manifold is conveniently expressed as the implicit condition  $g[\rho_{12}, \rho_{13}, \rho_{23}] = 0$ , where

$$g[\rho_{12}, \rho_{13}, \rho_{23}] = 2\rho_{12}\rho_{13}\rho_{23} - \rho_{12}^2\rho_{13}^2 - \rho_{12}^2\rho_{23}^2 - \rho_{13}^2\rho_{23}^2 + \rho_{12}^2\rho_{13}^2\rho_{23}^2. \quad (7)$$

This manifold is defined under the constraint  $g^* = 1 + 2\rho_{12}\rho_{13}\rho_{23} - \rho_{12}^2 - \rho_{13}^2 - \rho_{23}^2 > 0$ ; regions of the correlation space where  $g^* \leq 0$  correspond to parameter combinations for which  $\Omega$  is undefined. Indeed,  $g^* > 0$  is precisely the condition ensuring positive definiteness of the covariance matrix  $\mathbf{C}$  (App. A of [30]).

The partition of the correlation space defined by  $g=0$  can be visualized through two-dimensional slices at fixed  $\rho_{23}$ , as shown in Fig. 2(a,b). In these sections, the redundant regions form narrow, bow-tie-shaped domains corresponding to specific correlation motifs (indicated by the triangles), while synergistic behavior occupies the complementary, more extended portions of the correlation

space where  $g^* > 0$ . The symmetry of these slices under index permutations and even sign flips among the three correlation coefficients directly reflects the invariance of the O-information, as detailed in App. A of [30].

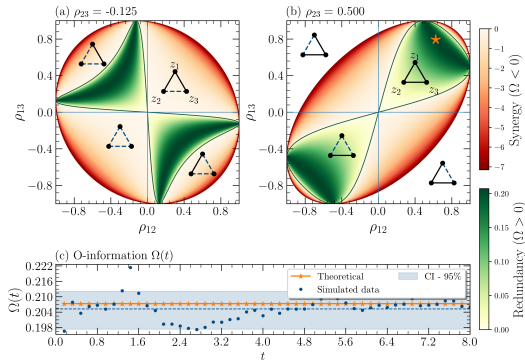


Figure 2. Phase diagram of redundancy (green) and synergy (red) in triplet correlation space. (a,b) Two-dimensional slices of the correlation space  $(\rho_{12}, \rho_{13}, \rho_{23}) \in [-1, 1]^3$  at fixed  $\rho_{23}$ , showing the sign of the O-information: redundant regions ( $\Omega > 0$ ) and synergistic regions ( $\Omega < 0$ ).  $\Omega$  is not defined in white regions where  $g^* \leq 0$ . Triangles show the sign of the pairwise environment-mediated correlations between the dynamical variables  $\{z_1, z_2, z_3\}$ . Positive correlations,  $\rho_{kl} > 0$ , between  $z_k$  and  $z_l$  are marked by continuous black edges. Dotted blue edges mark negative correlations. (c) O-information for a system with constant parameters ( $\mu = (0.5, 0.6, 0.4)$ ,  $\theta = (0, 0.25, 0.15)$  and  $\mathbf{f}(t) = \varphi = (0.2, 0.2, 0.2)$ ) yielding the correlations marked by a star in panel (b). The analytical prediction (stars) is compared with numerical simulations (circles). The mean and 95% confidence interval (CI) of the numerical simulations are indicated by the dashed line and shaded region, respectively.

A salient geometric consequence illustrated by the sections in Fig. 2 is that redundancy is more constrained than synergy. Redundant behavior arises only for specific sign patterns and magnitudes of the correlations: either when all correlations are positive,  $(\text{sgn}(\rho_{12}), \text{sgn}(\rho_{13}), \text{sgn}(\rho_{23})) = (+, +, +)$ , or when the system is predominantly anti-correlated, such as  $(-, -, +)$  and its permutations  $\mathcal{P}(-, -, +)$ .

In contrast, synergy is admissible for all sign combinations and is the *only* possible behavior in fully anti-correlated motifs  $(-, -, -)$  or in partially correlated arrangements of the form  $\mathcal{P}(+, +, -)$ . According to Harary's structural balance theory [33], these motifs are unbalanced: they contain cycles with a negative product of edge signs.

This observation agrees with the recent findings of Caprioglio et al. [34], who argued that unbalanced correlation structures are sufficient for synergy dominance in Gaussian systems. Our results further show that synergistic behavior can also arise in balanced correlation motifs with an even number of negative edges, such as  $\mathcal{P}(-, -, +)$ , although redundancy is also possible in these

structures.

Our analytical results further suggest that partially anti-correlated systems (sign motifs  $\mathcal{P}(-, -, +)$ ) may transition between redundancy and synergy as the correlation magnitudes vary, whereas partially correlated systems with  $\mathcal{P}(+, +, -)$  are intrinsically synergistic and never exhibit redundancy.

We now study the influence of local and shared environments on  $\Omega$  for systems with constant coupling to the shared environment (i.e., constant  $f_k(t) = \varphi_k$ ). In this case, Eq. (6) predicts a constant O-information whenever it is defined.

In terms of the local environment,  $\Omega$  becomes undefined when more than one  $\theta_k = 0$ , while only redundant behavior ( $\Omega \geq 0$ ) occurs when  $\theta_k = 0$  for a single variable (App. C in [30]). For instance, setting  $\theta_1 = 0$  leads to non-independent correlations satisfying  $\rho_{23} = \rho_{12}\rho_{13}$  and  $\Omega = -\frac{1}{2} \log_2 (1 - \rho_{23}^2) \geq 0$ .

With respect to the shared environment,  $\Omega = 0$  whenever  $\varphi_k = 0$  for any  $k$ , meaning no higher-order behavior is possible if fewer than three components of  $\mathbf{z}$  are coupled to the shared environment, as expected. Less intuitively, redundant behavior is the only possible outcome when all three dynamical variables are coupled to both the local and shared environments with *constant* nonzero coefficients  $\theta$  and  $\varphi$  (App. C in [30]).

Fig. 2(c) shows the results for the system with constant environmental couplings yielding the correlations marked by the star in Fig. 2(b). Redundant behavior is observed with  $\Omega = 0.207$ . Numerical simulations yield a fluctuating O-information  $\Omega(t) = 0.205[95\% \text{ CI } 0.197 - 0.212]$  consistent with the analytical prediction (cf. stars and circles in Fig. 2(c)).

Next, we consider time-dependent couplings  $f_k(t) = \varphi_k t^{\alpha_k} e^{-\beta_k t}$  with  $\alpha_k \geq 0$ , and  $\beta_k \geq 0$ , for  $k \in \{1, 2, 3\}$ . This functional form of  $f_k(t)$  encompasses a broad class of time-varying coupling profiles commonly observed in complex systems [35, 36].

Our analysis reveals an important finding: *time-dependent coupling to a shared environment can induce redundancy-to-synergy transitions*. Fig. 3 illustrates this behavior for a system with varying couplings  $f_2(t)$  and  $f_3(t)$  (panel (a)), which drive a dynamical evolution within correlation space (panel (b)).  $\Omega(t)$  transitions from positive (redundant) to negative (synergistic) values over time, as shown by both analytical predictions and numerical simulations. The excellent agreement between theory and simulations is further documented in App. D of [30], where we compare the time evolution of the mean vector  $\mathbf{M}$  and covariance matrix  $\mathbf{C}$  obtained from analytical and numerical results.

*Combined effect of environmental coupling and deterministic interactions.*— Our numerical simulations reveal a rich phenomenology arising from the interplay between environmental coupling and deterministic interactions, quantified by  $f_k(t)$  and  $m(\mathbf{z})$ , respectively. Fig. 4

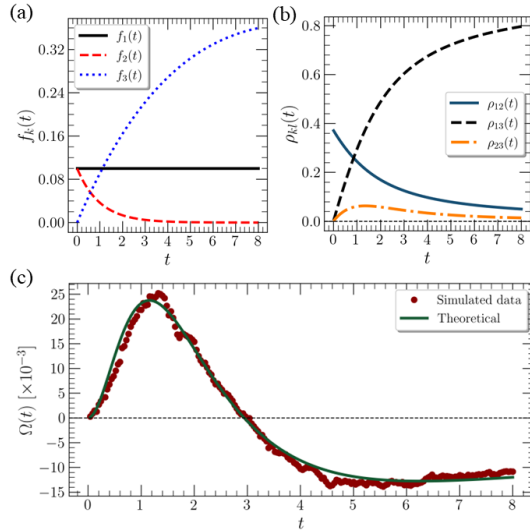


Figure 3. System with time-varying coupling to the shared environment. (a) Temporal variation of the coupling strength to the shared environment for each variable, as indicated in the legend. (b) Time evolution of the pairwise correlation coefficients. (c) Analytical and numerical results for the O-information. Simulations were run with parameters  $\mu = (0.5, 0.6, 0.4)$ ,  $\theta = (0, 0.1, 0.1)$ ,  $\varphi = (0.1, 0.1, 0.1)$ ,  $\alpha = (0, 0, 1)$  and  $\beta = (0, 1, 0.1)$ , using  $2 \times 10^4$  trajectories, and  $4 \times 10^3$  time steps.

illustrates the time evolution of  $\Omega(t)$  for a system interacting with a shared environment that favors redundancy (indicated by the solid horizontal line), under different choices of the deterministic interaction parameters  $m(\mathbf{z})$ . Several key observations emerge.

First, a nonzero  $\Omega(t)$  arises even with only low-order deterministic interactions (i.e., for  $m_1, m_2 \neq 0$  with  $m_3 = 0$ ), consistent with our earlier result that environmental coupling alone can generate collective dependencies.

Second, although a positive third-order interaction ( $m_3 > 0$ ) would, in the absence of a shared environment, favor redundancy, this intuition no longer holds in the presence of environmental coupling. Indeed,  $\Omega(t)$  can decrease over time, indicating a transient reduction in redundancy despite  $m_3 > 0$  (stars in Fig. 4(a)).

Third, nonzero deterministic interactions ( $m(\mathbf{z}) \neq 0$ ) enable redundancy–synergy transitions even when the environmental couplings favor redundancy. This is illustrated in Figure 4(b) for negative deterministic interactions.

Remarkably, synergy can emerge not only from higher-order interactions ( $m_3 < 0$ ) but also from low-order deterministic terms with negative  $m_1$  or  $m_2$ . The effect is even stronger and occurs earlier in these low-order cases, suggesting that synergy may emerge from the interplay between redundancy-dominated environmental coupling and low-order deterministic interactions, even without explicit higher-order terms.

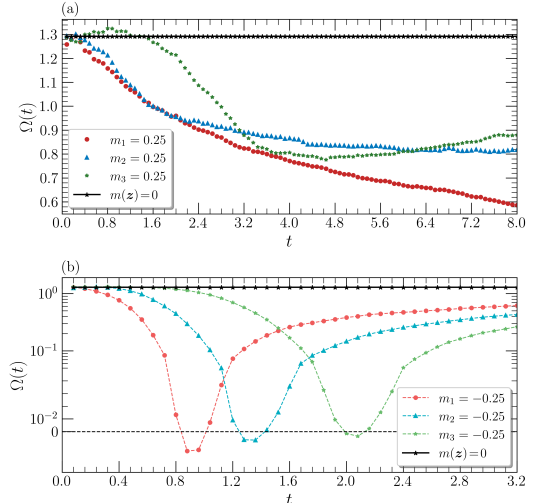


Figure 4. Effect of deterministic interactions on the behavior of systems with *constant* coupling to a shared environment. Time evolution of the O-information for several values of the deterministic couplings  $m_1$ ,  $m_2$ , and  $m_3$ , indicated by the symbols in the legends. Panels (a) and (b) correspond to positive and negative values of the deterministic couplings, respectively. The solid black lines show a baseline for  $\Omega(t)$  defined by the corresponding systems without deterministic interactions (i.e., with  $m(\mathbf{z}) = 0$ ). Simulations were run with parameters  $\mu = (0.5, 0.6, 0.4)$ ,  $\theta = (0, 0.25, 0.15)$  and  $\mathbf{f}(t) = \varphi = (0.2, 0.6, 1)$ , using  $2 \times 10^4$  trajectories, and  $4 \times 10^3$  time steps.

*Conclusions.*— We have shown that higher-order collective behavior can emerge purely from shared stochastic environments, even in the absence of direct interactions among constituent units. While redundancy occupies narrow regions of correlation space, environment-induced synergy appears more prevalent, though it requires time-dependent coupling to the shared environment. These findings uncover an alternative pathway to collective organization, extending the traditional interaction-based framework of complex systems.

Beyond stochastic effects alone, we find a rich phenomenology arising from the interplay between environmental coupling and deterministic interactions, with nontrivial transitions between redundant and synergistic regimes. Importantly, the coexistence of distinct mechanisms that can give rise to similar collective behavior implies that observations alone may be insufficient to identify their origin. This highlights the need for methods capable of disentangling environmental and interaction-driven contributions, a distinction that may be crucial for controlling collective behavior in complex systems.

*Acknowledgments.*— This research was funded by the BBSRC grant no. BB/Y513027/1.

*Data availability.*— The data that support the findings of this article are publicly available [37].

---

\* felipe.abrilbermudez@abdn.ac.uk  
 † david.fisher@abdn.ac.uk  
 ‡ jbgramain@abdn.ac.uk  
 § fperez-reche@abdn.ac.uk

- [1] M. E. J. Newman, *American Journal of Physics* **79**, 800 (2011).
- [2] J. Ladyman and K. Wiesner, *What Is a Complex System?* (Yale University Press, 2020).
- [3] P. W. Anderson, *Science* **177**, 393 (1972).
- [4] N. Goldenfeld and L. P. Kadanoff, *Science* **284**, 87 (1999).
- [5] H. Matsuda, *Phys. Rev. E* **62**, 3096 (2000).
- [6] T. Squartini, G. Caldarelli, G. Cimini, A. Gabrielli, and D. Garlaschelli, *Physics Reports* **757**, 1 (2018).
- [7] B. Prasse and P. V. Mieghem, *Proceedings of the National Academy of Sciences of the United States of America* **119**, e2205517119 (2022).
- [8] F. Battiston, E. Amico, A. Barrat, G. Bianconi, G. F. de Arruda, B. Franceschiello, I. Iacopini, S. Kéfi, V. Latora, Y. Moreno, M. M. Murray, T. P. Peixoto, F. Vaccarino, and G. Petri, *Nat. Phys.* **17**, 1093–1098 (2021).
- [9] D. Marinazzo, *Physics* **18**, 10.1103/PHYSICS.18.71 (2025).
- [10] M. E. J. Newman, *Networks: an introduction* (Oxford University Press, 2010).
- [11] S. N. Dorogovtsev and J. F. F. Mendes, *The nature of complex networks* (Oxford University Press, 2022).
- [12] A. B. Barrett, *Phys. Rev. E* **91**, 10.1103/physreve.91.052802 (2015).
- [13] F. E. Rosas, P. A. M. Mediano, M. Gastpar, and H. J. Jensen, *Phys. Rev. E* **100**, 10.1103/physreve.100.032305 (2019).
- [14] S. Stramaglia, T. Scagliarini, B. C. Daniels, and D. Marinazzo, *Front. Physiol.* **11**, 10.3389/fphys.2020.595736 (2021).
- [15] T. Scagliarini, D. Marinazzo, Y. Guo, S. Stramaglia, and F. E. Rosas, *Phys. Rev. Res.* **4**, 10.1103/physrevresearch.4.013184 (2022).
- [16] M. J. Silk, M. Q. Wilber, and N. H. Fefferman, *Ecology Letters* **25**, 2217 (2022).
- [17] T. Gibbs, S. A. Levin, and J. M. Levine, *Proceedings of the National Academy of Sciences of the United States of America* **119**, e2205063119 (2022).
- [18] L. Gallo, L. Lacasa, V. Latora, and F. Battiston, *Nat. Comm.* **15**, 10.1038/s41467-024-48578-6 (2024).
- [19] A. Civilini, O. Sadekar, F. Battiston, J. Gómez-Gardeñes, and V. Latora, *Physical Review Letters* **132**, 167401 (2024).
- [20] T. Robiglio, M. Neri, D. Coppes, C. Agostinelli, F. Battiston, M. Lucas, and G. Petri, *Phys. Rev. Lett.* **134**, 10.1103/physrevlett.134.137401 (2025).
- [21] A. P. Millán, H. Sun, L. Giambagli, R. Muolo, T. Carletti, J. J. Torres, F. Radicchi, J. Kurths, and G. Bianconi, *Nature Physics* **2025** 21:3 **21**, 353 (2025).
- [22] F. J. Pérez-Reche and S. N. Taraskin, *Physical Review E* **112**, L032301 (2025).
- [23] J. N. Teramae and D. Tanaka, *Physical Review Letters* **93**, 204103 (2004).
- [24] M. Sireci, M. A. Muñoz, and J. Grilli, *Proceedings of the National Academy of Sciences* **120**, e2217144120 (2023).
- [25] A. Taitelbaum, R. West, M. Mobilia, and M. Assaf, *Physical Review Research* **5**, L022004 (2023).
- [26] D. A. Vasseur and J. W. Fox, *Nature* **2009** 460:7258 **460**, 1007 (2009).
- [27] R. Moreno-Bote, J. Beck, I. Kanitscheider, X. Pitkow, P. Latham, and A. Pouget, *Nature Neuroscience* **2014** 17:10 **17**, 1410 (2014).
- [28] A. Onuki, *Phase transition dynamics* (Cambridge University Press, 2007) p. 714.
- [29] D. T. Gillespie, *Am. J. Phys.* **64**, 1246 (1996).
- [30] (2025), see Supplemental Material at [URL by publisher] for detailed derivations and additional results.
- [31] P. E. Kloeden and E. Platen, *Numerical Solution of Stochastic Differential Equations* (Springer Berlin Heidelberg, 1992) doi: <http://dx.doi.org/10.1007/978-3-662-12616-5>.
- [32] M. Neri, D. Vinchhi, C. Ferreyra, T. Robiglio, O. Ates, M. Ontivero-Ortega, A. Brovelli, D. Marinazzo, and E. Combrisson, *Journal of Open Source Software* **9**, 7360 (2024).
- [33] F. Harary, *Michigan Mathematical Journal* **2**, 143 (1953).
- [34] E. Caprioglio, P. A. M. Mediano, and L. Berthouze, *Synergistic motifs in gaussian systems* (2025).
- [35] S. Bhandary, D. Biswas, T. Banerjee, and P. S. Dutta, *Physical Review E* **106**, 10.1103/physreve.106.014309 (2022).
- [36] D. J. Fenn, M. A. Porter, S. Williams, M. McDonald, N. F. Johnson, and N. S. Jones, *Phys. Rev. E* **84**, 10.1103/physreve.84.026109 (2011).
- [37] F. Abril, GitHub repository (2025), [https://github.com/fsabrilb/0\\_information\\_toy\\_model](https://github.com/fsabrilb/0_information_toy_model).